

## Photoluminescence properties of porous silicon layers prepared by electrochemical etching in extremely dilute HF solutions

HIDEKI KOYAMA

*Department of Practical Life Studies, Technology Education Group, Hyogo University of Teacher Education, Yashiro, Hyogo 673-1494, Japan*

*(tel.: +81-795-44-2174, fax: +81-795-44-2174, e-mail: koyama@life.hyogo-u.ac.jp)*

Received 15 August 2005; accepted in revised form 20 March 2006

*Key words:* anodization, etching, nanocrystal, nanostructure, photoluminescence, porous silicon

### Abstract

Dilute HF solutions with concentrations down to 0.03% have been used to obtain luminescent porous silicon (PSi) layers on p-type Si wafers. The experimental results show that with a constant etching time of 30 min, PSi layers with sufficient luminescence efficiencies can be formed for HF concentrations as low as 0.1%. Because of a significantly lowered critical current density, only very low etching current densities of  $\leq 0.1 \text{ mA cm}^{-2}$  can result in the formation of luminescent PSi samples in 0.1% HF solutions. A notable result is that these low etching current densities cannot be used to form luminescent PSi layers in concentrated ( $\geq 1\%$ ) HF solutions. The behavior of PL intensity as a function of etching current density has been analyzed over a wide range of HF concentration. The PL intensity is determined by the ratio of the etching current density to the critical current density, suggesting that the presence of silicon oxides plays an important role in the formation of luminescent Si nanostructures in PSi layers.

### 1. Introduction

The observation of efficient, room-temperature visible photoluminescence (PL) from porous silicon (PSi) by Canham [1] has triggered a vast number of experimental and theoretical studies on this novel optoelectronic material [2, 3]. PSi layers are made by electrochemically etching Si wafers in HF solutions [4, 5]. Since the basic structure of highly luminescent PSi is a random network of nanosize Si skeletons, quantum confinement of carriers is suggested to play a vital role in the visible PL of this material [6]. Evidence of deeply localized states has also been observed experimentally in air-exposed samples [7], and the effect of double-bonded oxygen has been discussed [8]. PSi-based light emitting diodes now exhibit efficiencies higher than 1% [9]. PSi is also a promising material in a wide area of applications including waveguides [10], dielectric mirrors/filters [11, 12], polarization optics components [13, 14], chemical/biological sensors [15, 16], photoelectrochemical/photo-voltaic devices [17, 18], field electron emitters [19], and ultrasound devices [20].

In most cases, PSi layers are prepared by using concentrated, 10–50% HF solutions. There are, however, application areas of PSi layers in which the use of such concentrated HF solutions should be avoided. These may include PSi-based educational tools [21], because concentrated HF solutions are too toxic to be

used in classrooms. Nevertheless, only a few attempts to date have been performed to obtain PSi layers with dilute HF solutions (<10%) [22–24]. These previous studies, however, aimed at investigating the formation mechanism of PSi layers and not at producing luminescent ones. In fact, no luminescence data were reported in these papers.

In this study, we have investigated the PL properties of the PSi layers prepared with various HF solutions of a wide range (0.03–30%) of HF concentrations. The results show, for the first time to our knowledge, that sufficiently luminescent PSi layers can be obtained for extremely low HF concentrations as low as 0.1%. Because of lowered critical current densities, these dilute HF solutions can produce PSi layers only with very low anodization current densities. A noticeable finding is that such low anodization current densities cannot be used to form luminescent PSi layers in concentrated HF solutions. The formation mechanism of luminescent nanoporous layers is discussed based on the behavior of the PL intensity as a function of HF concentration and etching current density.

### 2. Experimental details

Single-crystal Si (100) wafers of p-type, 0.01–0.02  $\Omega \text{ cm}$  were anodically etched in aqueous HF solutions with

HF concentrations in the range of 0.03–30%. These HF solutions were prepared by mixing 55% HF with pure water. Anodization was performed in the dark for a fixed anodization time of 30 min. The etched samples were then rinsed with ethanol and blown dry.

PL spectra were measured at room temperature under the excitation by a laser diode at  $\lambda = 410$  nm ( $h\nu = 3.02$  eV). A fiber-optic spectrometer (Ocean Optics USB2000) was used. The resolution of the spectrometer was  $\sim 4$  nm. For each PSi sample, we took five PL spectra on different spots on the sample surface. Each PL spectrum shown below is the average of five spectra obtained in this way. All the PL spectra shown here are corrected for apparatus response.

### 3. Results and discussion

#### 3.1. Critical current densities

Figure 1 summarizes the measurements of PL intensities for various PSi samples prepared with different HF solutions and etching current densities. In this figure, the measured PL intensities are graded into five levels and plotted with circles of different size. Crosses indicate PSi samples suffered from partial or total electropolishing. The experimental data show that luminescent PSi samples with detectable PL intensities can be obtained for HF concentrations in the range of 0.1–10%. At a higher HF concentration of 30%, only low-porosity, non-luminescent PSi layers were formed. For the HF concentration of 0.03% we could not even find any PSi layers on the etched surfaces by the naked eye.

For a fixed HF concentration, the PL intensity increases monotonically with increasing etching current density. This can be attributed to the fact that the porosity of the PSi layer in general increases with

etching current density [25, 26]. However, too great an increase in current density causes partial or total dissolution of the layers due to electropolishing [4, 5]. This implies that the most highly luminescent, uniform PSi layers should be formed at current densities just below the onset of the electropolishing regime, which is consistent with the results of Figure 1.

Several groups have measured the critical current density between the PSi-formation and electropolishing regimes as a function of HF concentration [22, 23], and their results are also shown by dashed or dotted lines in Figure 1. These data were obtained from the positions of characteristic structures in the current–voltage curves of Si electrodes in HF solutions. Zhang et al. [22] have defined two critical current densities, one corresponding to the maximum slope and the other to the first peak ( $J_1$ ) of the current–voltage curve. These two critical current densities define the transition regime in which partial electropolishing occurs. Lehmann [23] has measured  $J_1$  for HF concentrations from 1 to 10% and derived a formula

$$J_1(C_{\text{HF}}) = AC_{\text{HF}}^{1.5} \quad (1)$$

where  $C_{\text{HF}}$  is the HF concentration of the solution and  $A$  is a temperature-dependent coefficient. The dashed line in Figure 1 shows the values for  $J_1$  extrapolated based on Equation (1). As seen from Figure 1, the lower critical current density reported by Zhang et al. seems to describe best the onset of the electropolishing regime in our experimental data.

The critical current density significantly decreases as HF concentration is decreased. This is because the rate of dissolution of Si oxides slows down at low HF concentrations [22]. The low dissolution rate of Si oxides reduces the possibility for Si to dissolve directly into the solution, which is necessary for PSi layers to be formed. Thus in order to form PSi layers at low HF concentrations, anodic etching must be done at lower current densities to control the formation of Si oxides. According to our result shown in Figure 1, PSi layers can be formed only with those etching current densities of  $\leq 0.1$  mA cm $^{-2}$  in 0.1% HF. In concentrated solutions ( $\geq 1\%$ ), no luminescent PSi layers can be formed with these low etching current densities. This implies that the use of dilute HF solutions has another advantage: it enables us to form luminescent PSi layers at very small rates to obtain very thin layers of luminescent PSi with a better control of thickness.

#### 3.2. PL spectra

Measured PL spectra of our PSi samples are shown in Figures 2 and 3. In Figure 2, we show the spectra of the most highly luminescent PSi samples for respective HF concentrations. Significant interference fringes were observed in samples made with 3 and 10% HF solutions. Figure 3 shows the PL spectra of PSi samples prepared with 0.1% HF. All of these spectra exhibit the

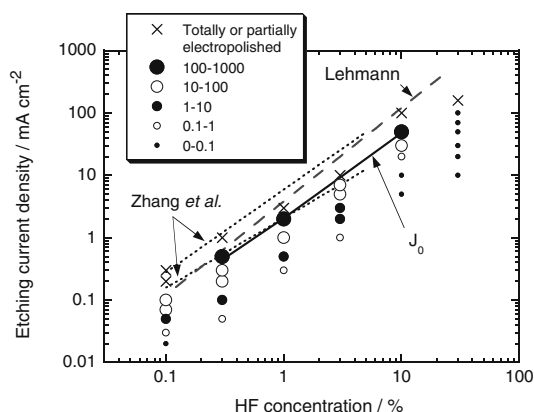


Fig. 1. Summary of the PL intensity measurements performed on PSi samples prepared with different etching current densities and HF concentrations. The measured PL intensities, being in the range of 0–1000 in our units, are shown by circles of different size according to the criteria shown in the inset. Crosses indicate samples suffered from partial or total electropolishing. The dotted and dashed lines show the critical current densities reported by Zhang et al. [22] and Lehmann [23], respectively. The solid line shows the critical current densities obtained in this study based on Equation (2).

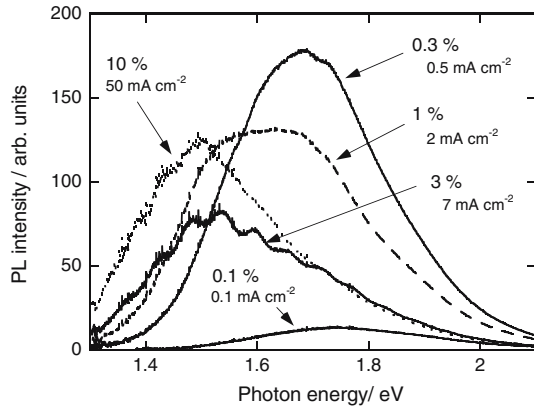


Fig. 2. PL spectra of five PSi samples prepared with different HF solutions. These PSi samples, formed at the etching current densities indicated, are the most highly luminescent ones among those prepared with the same HF solution.

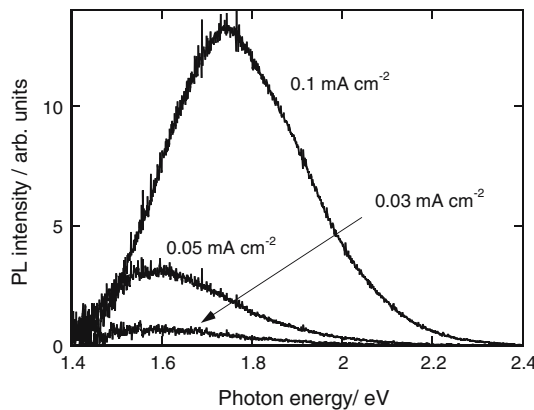


Fig. 3. PL spectra of three PSi samples prepared in 0.1% HF with different current densities.

broad and Gaussian lineshape, suggesting that these emissions originate from the same mechanism. As shown in Figure 2, the most highly luminescent samples exhibit similar PL intensities except for the one made with 0.1% HF. The low PL intensity observed in the sample etched in 0.1% HF is presumably due to its insufficient thickness, since an estimation based on the charge density passed during the electrochemical etching yields a thickness of the order of 100 nm. The PL intensity of this sample, nevertheless, is such that its orange emission can be seen clearly under ambient light with an excitation power of  $\sim 1$  mW over a  $1 \text{ mm}^2$  spot.

### 3.3. Emission intensity

The behavior of PL intensity as a function of etching current density is shown in Figure 4 for different HF concentrations. The PL intensity ( $I$ ) increases superlinearly with increasing etching current density ( $J$ ), which is consistent with other reports [27, 28]. Our experimental results further show that this behavior can be described by a power law

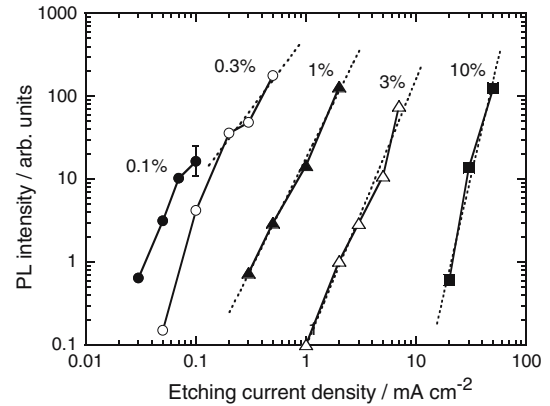


Fig. 4. PL intensities of PSi samples plotted as a function of etching current density. The dotted lines show the best fits of Equation (2).

$$I(J) = I_0 \left[ \frac{J}{J_0(C_{\text{HF}})} \right]^{\gamma(C_{\text{HF}})} \quad (2)$$

over a wide range of HF concentration. Here  $I_0$  represents the PL intensity when  $J = J_0$ . Thus if we assign  $I_0$  the PL intensity of the most highly luminescent sample at some HF concentration,  $J_0$  should give the critical current density at that HF concentration. This is because the highest PL intensity is observed in a PSi sample etched at a current density very close to the critical current density, as shown in Figure 1. Since the PL intensities of these highly luminescent PSi samples are similar for HF concentrations in the range of 0.3–10%, as shown in Figures 2 and 4, we assume  $I_0$  to be independent of  $C_{\text{HF}}$  and take the average PL intensity value of 128 (in our units) for this constant. Then, the best fits of Equation (2), shown by the dotted lines in Figure 4, give  $J_0$  values as shown by the solid line in Figure 1. In these fitting calculations, we did not use the PL intensities of PSi samples prepared at current densities equal to or less than  $0.1 \text{ mA cm}^{-2}$ , because of their insufficient thickness. The  $J_0$  values obtained by these fitting calculations coincide well with the current densities at which the most highly luminescent samples are formed, and are close to the lower critical current densities reported by Zhang et al. [22]. These  $J_0$  values can be fitted by a power law of  $J_0 \propto C_{\text{HF}}^{1.34}$ . The exponent  $\gamma$  in Equation (2), also obtained by the fitting calculations, are shown in Figure 5 as a function of  $C_{\text{HF}}$ . These values for  $\gamma$  seem to make another power dependence of  $\gamma(C_{\text{HF}}) = 2.57 C_{\text{HF}}^{0.32}$  as shown by the solid line.

In Equation (2), the effect of etching current density on the PL intensity only appears through the ratio  $J/J_0$ . This implies that the formation of luminescent Si nanostructures is not governed solely by the electronic processes that depend on the absolute current density  $J$ , such as field-induced processes [26] or carrier diffusion [29]. Instead, Equation (2) suggests that the relative rates of two competing dissolution mechanisms are important: tetravalent dissolution via the formation of silicon oxides and divalent direct dissolution. The rate of the former reaction increases rapidly as  $J$  approaches  $J_0$

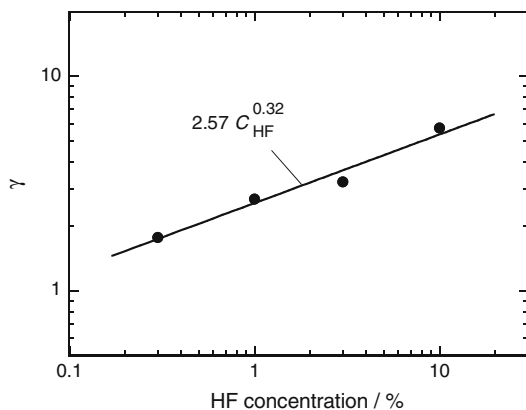


Fig. 5. Values for  $\gamma$  obtained by fitting Equation (2) to the data of Figure 4. The solid line shows a power function that fits best to the data.

[23], and this behavior seems to correspond to that of the PL intensity as shown in Figure 4. Thus it can be concluded that the formation of silicon oxides plays a major role in producing luminescent Si nanostructures in PSi layers. This hypothesis is supported further by the experimental results of Propst et al. [30]. They used non-oxidative, anhydrous HF solutions to obtain PSi layers. Their microscopic analyses found no detectable amount of Si nanostructures in the PSi layers. An oxide layer formed at a pore tip can hinder the stable growth of the pore, enabling etching reactions to occur at its side wall [22]. This will reduce the interpore spacing or cause a random propagation of pores, either of which may lead to the formation of nanostructures. There is, however, some variation in  $\gamma$  as a function of  $C_{HF}$  as shown in Figure 5. This indicates that the contribution by the electric field or carrier diffusion is not negligible.

### 3.4. Emission photon energy

The emission photon energies of PSi samples are plotted in Figure 6 for respective HF concentrations as a function of etching current density. The emission energy shows anomalous behavior with increasing etching current density: it shows a large redshift for 3 or 10% HF while an apparent blueshift is recognized for 0.1 or

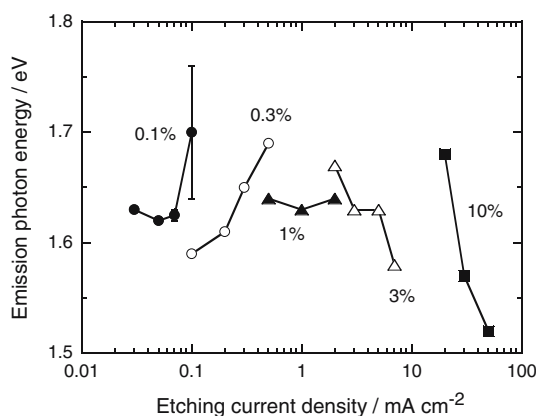


Fig. 6. Peak PL photon energies of PSi samples plotted vs. etching current density.

0.3% HF. Neither of the redshifts turn to a blueshift even though data from partially electropolished samples prepared at much higher etching current densities are included. In many cases the emission from PSi shows a blueshift with increasing etching current density [31]. This is consistent with the quantum confinement hypothesis, because the porosity in general increases with increasing current density [25, 26]. For  $n^+$ -Si a large decrease in porosity is reported [32]. However, to our knowledge there is no published data demonstrating any decrease in porosity with increasing etching current density for p-type Si wafers. Detailed microscopic analyses need to be carried out before we further discuss the origin of the large redshift. What we should note here is that our experimental data in Figure 6 show another advantage of using dilute HF solutions for the preparation of luminescent PSi samples: it can efficiently produce luminescent samples emitting at higher photon energies than concentrated HF solutions do.

## 4. Conclusion

We have shown that luminescent PSi layers can be formed by anodic etching in HF solutions with HF concentrations as low as 0.1%. This result may facilitate the use of PSi layers for educational purposes. Because of a remarkably lowered critical current density, only those etching current densities equal to or less than  $0.1 \text{ mA cm}^{-2}$  successfully resulted in the formation of efficiently luminescent PSi layers in 0.1% HF. These extremely low current densities never result in the formation of luminescent PSi layers in concentrated ( $\geq 1\%$ ) HF solutions. This suggests another advantage of using dilute HF solutions, i.e., it can produce very thin layers of luminescent PSi layers with a better control of thickness. Analyses of the PL intensity as a function of etching current density have revealed that the PL intensity depends on the ratio of the etching current density to the critical current density. This implies that the formation of silicon oxides plays an important role in producing luminescent Si nanostructures.

## Acknowledgements

This work was supported in part by a research grant from Hyogo Science and Technology Association and by a Grant-in-Aid for Scientific Research from the Japan Society for the Promotion of Science.

## References

1. L.T. Canham, *Appl. Phys. Lett.* **57** (1990) 1046.
2. D.J. Lockwood, *Solid State Commun.* **92** (1994) 101.
3. A.G. Cullis, L.T. Canham and P.D.J. Calcott, *J. Appl. Phys.* **82** (1997) 909.

4. A. Uhlir Jr., *Bell Syst. Tech. J.* **35** (1956) 333.
5. D.R. Turner, *J. Electrochem. Soc.* **105** (1958) 402.
6. A.G. Cullis and L.T. Canham, *Nature* **353** (1991) 335.
7. H. Koyama, N. Shima and N. Koshida, *Phys. Rev. B* **53** (1996) R13291.
8. M.V. Wolkin, J. Jorne, P.M. Fauchet, G. Allan and C. Delerue, *Phys. Rev. Lett.* **82** (1999) 197.
9. B. Gelloz and N. Koshida, *J. Appl. Phys.* **88** (2000) 4319.
10. V.P. Bondarenko, A.M. Dorofeev and N.M. Kazuchits, *Microelectron. Eng.* **28** (1992) 447.
11. G. Vincent, *Appl. Phys. Lett.* **64** (1994) 2367.
12. L. Pavesi and C. Mazzoleni, *Appl. Phys. Lett.* **67** (1995) 2983.
13. D. Kovalev, G. Polisski, J. Diener, H. Heckler, N. Künzner, V.Yu. Timoshenko and F. Koch, *Appl. Phys. Lett.* **78** (2001) 916.
14. H. Koyama, *J. Appl. Phys.* **96** (2004) 3716.
15. R.L. Smith and D.C. Scott, *IEEE Trans. Biomed. Eng.* **BME-33** (1986) 83.
16. K.-P.S. Dancil, D.P. Greiner and M.J. Sailor, *J. Am. Chem. Soc.* **121** (1999) 7925.
17. N. Koshida, H. Koyama and Y. Kiuchi, *Jpn. J. Appl. Phys.* **25** (1986) 1069.
18. B. Ünal and S.C. Bayliss, *J. Appl. Phys.* **80** (1996) 3532.
19. N. Koshida, T. Ozaki, X. Sheng and H. Koyama, *Jpn. J. Appl. Phys.* **34** (1995) L705.
20. H. Shinoda, T. Nakajima, K. Ueno and N. Koshida, *Nature* **400** (1999) 853.
21. V.P. Parkhutik and L.T. Canham, *Phys. Stat. Sol. (a)* **182** (2000) 591.
22. X.G. Zhang, S.D. Collins and R.L. Smith, *J. Electrochem. Soc.* **136** (1989) 1561.
23. V. Lehmann, *J. Electrochem. Soc.* **140** (1993) 2836.
24. A. Belaïdi, M. Safi, F. Ozanam, J.-N. Chazalviel and O. Gorochoy, *J. Electrochem. Soc.* **146** (1999) 2659.
25. G. Bomchil, R. Herino, K. Barla and J.C. Pfister, *J. Electrochem. Soc.* **130** (1983) 1611.
26. M.I.J. Beale, N.G. Chew, M.J. Uren, A.G. Cullis and J.D. Benjamin, *Appl. Phys. Lett.* **46** (1985) 86.
27. T. Ban, T. Koizumi, S. Haba, N. Koshida and Y. Suda, *Jpn. J. Appl. Phys.* **33** (1994) 5603.
28. M. Ohmukai and Y. Tsutsumi, *Jpn. J. Appl. Phys.* **36** (1997) L292.
29. R.L. Smith, S.-F. Chuang and S.D. Collins, *J. Electron. Mater.* **17** (1988) 533.
30. E.K. Propst, M.M. Rieger, K.W. Vogt and P.A. Kohl, *Appl. Phys. Lett.* **64** (1994) 1914.
31. N. Koshida and H. Koyama, *Jpn. J. Appl. Phys.* **30** (1991) L1221.
32. A. Halimaoui, in L. Canham (ed.), 'Properties of Porous Silicon', EMIS Datareviews Series no.18 (IEE INSPEC, London, 1991), p.12.